An Analog-digital CMOS circuit for motion detection based on direction-selective neural networks

Masato Koutani, Tetsuya Asai, and Yoshihito Amemiya

Department of Electrical Engineering, Hokkaido University

Kita 13, Nishi 8, Kita-ku, Sapporo, 060-8628, Japan.

Abstract

We have developed a compact CMOS motion-detection circuit based on a direction-selective neural-network architecture. The circuit consists of asynchronous current-mode digital subcircuits for edge detection and subthreshold analog subcircuits for motion-detection. SPICE and numerical simulations of the network show that the circuit can successfully extract edge lines from incident images and compute the two-dimensional local velocity of the image motion from the movement of the edge lines. The circuit is useful for constructing small-sized, low-power vision processing systems.

1 Introduction

One of the promising areas of research in vision electronics is the development of compact, practical motion-detection devices modeled after the mechanism of biological vision. This paper proposes one such promising device, an analog-digital hybrid CMOS circuit that performs motion detection by means of the direction-selective neural network architecture.

Ordinary motion-detection is performed by the calculation of an optical flow field. The optical flow field of an incident image is calculated at regular time intervals, then a motion vector field is estimated from the calculated data of the optical flow field. Practical vision algorithms [1, 2] and electronic vision circuits [3, 4, 5] for the motion detection have been developed. This approach is orthodox and easy to combine with other picture processing. However, it requires a large-scale processing hardware and, therefore, cannot be used for constructing compact, low-power systems.

Recently, bio-inspired LSIs based on *neuromorphic engineering* have been investigated in the literature [6, 7, 8]. Biological vision systems perform motion detection in a quite different (but very effective) way. The insect neuro-optical system, for instance, uses $medulla$ as a small spatial-field motion detector. It detects local-field motion with a $lobula\text{-}plate$ (an organ having large directional selectivity to motion) and aggregates the local motion data with a $lobula\text{-}complex$ (an organ that includes many $lobula\text{-}plates$ as constituent elements) to detect wide-field motion [9]. This fact implies that we can implement effective motion detection by combining the following procedures: i) detection of local motion at an early stage and ii) aggregation of the local motions at the subsequent stage. After the development of the model of such a biological vision system, a number of $neuromorphic\ vision\ chips$ have recently been studied and developed [6, 7, 8, 10]. The vision chips (modeled after the mechanism of biological vision) will certainly be in great demand in the future as powerful visual pre-processors because of their capability of parallel and real-time operations.

Aiming at the development of practical motion-detection systems based on the biological approach, we have developed an analog-digital hybrid CMOS circuit that implements a motion-detection network and a direction-selective neural network. The proposed circuits detect local motion by using subthreshold analog CMOS subcircuits designed for implementing a biological correlation neural network. The detected local motions are aggregated in a successive subcircuit to form wide-field direction-selective neural fields. For practical use of the motion-detection system, we also developed additional subcircuits for noise removal, quantization, and edge detection.

This paper is organized as follows. In Sect. 2, we first illustrate preprocessing required for motion detection, then introduce bidirectional correlation networks that respond to bidirectional motion of visual targets. In Sect. 3, we propose a model of direction-selective neural networks that uses the correlation networks. The CMOS circuits for implementing the preprocessing and the correlation neural networks are proposed in Sect. 4. Section 5 shows the operation of the proposed circuits and models. Section 6 is devoted to summary.

2 Motion detection with correlation neural networks

A correlation neural network (CNN) [11, 12, 13], which accounts for velocity sensitive responses of neurons, is suitable for analog circuit implementation of motion-detection systems and has been successfully implemented on CMOS LSIs [14, 15, 16, 17]. The CNN utilizes local motion detectors to correlate signals sampled at one location in the image with those sampled after a delay at adjacent locations,however, an edge-detection process is required in practical motion-detection systems with the CNNs [16, 18]. In this section, we introduce a compact edge-detection circuit that has current-mode input-output interfaces. Then, we in-

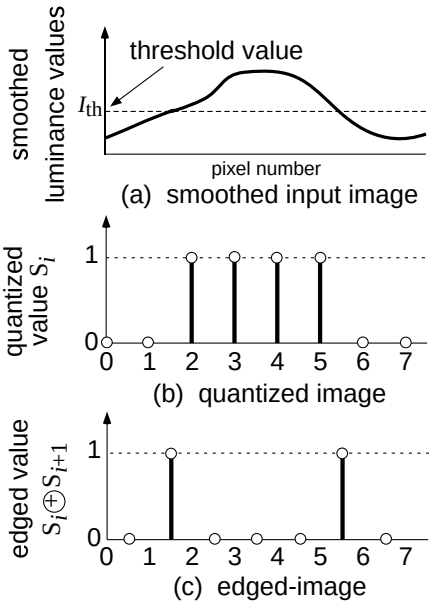

Figure 1: A simple edge-detection scheme for a motion-detection system: (a) luminance distribution of an input light; (b) quantized distribution of the input light with a given threshold value in (a); and (c) edged distribution obtained from the quantized distribution in (b).

troduce a subthreshold analog CMOS circuit for the motion detection.

The edge detection is performed by the following three processes: (i) an image smoothing for noise removal, (ii) a quantization of input images, and (iii) an exclusive OR (XOR) operation of the quantized images for the edge detection (Fig. 1). The smoothed luminance values of pixels in the input image [Fig. 1(a)] are quantized to logical "0" or logical "1" around the given threshold value [Fig. 1(b)]. Then, an edged-image is obtained by the XOR operation between the neighboring quantized values [Fig. 1(c)].

Figure 2 shows a primitive CNN for local motion detection. The network consists of (i) signal receptors (SRs) that receive the edged-images produced by the XOR operation, (ii) a delay neuron (D), and (iii) a correlator (C) that correlates the adjacent output of the signal receptor and the delay neuron. In Fig. 2, an output of the $(i-1)$-th signal receptor (SR_{i-1}) is sent to a delay neuron (D_{i-1}) that produces a delayed signal. An output of the i-th correlator C_i ($V_{\mathrm{out},i}$) is given by correlation values between (D_{i-1}) and (SR_i). The output of the correlator ($V_{\mathrm{out},i}$) depends on the velocity of the edge moving from SR_{i-1} to SR_i; in consequence, we can obtain the local velocity signal by the CNN structure. On the other hand, if the edge moves in the opposite direction (SR_i to SR_{i-1}), the output $V_{\mathrm{out}i}$, becomes zero because the delay mechanism decreases the correlation between the delayed signal (D_{i-1}) and undelayed signal(SR_i). Namely, the primitive CNN responds to only one direction (from SR_{i-1} to SR_i in Fig. 2).

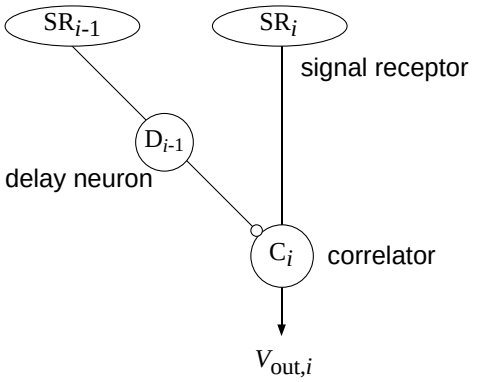

Figure 2: A primitive CNN for local-motion detection.

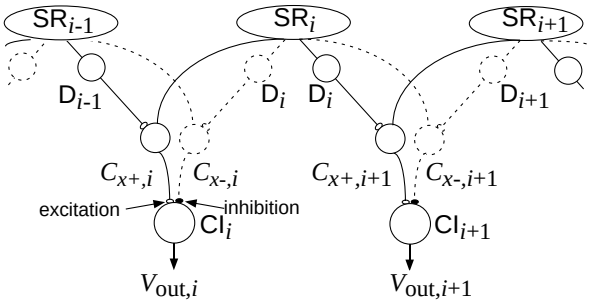

Figure 3: Bidirectional CNNs consisting of two primitive CNNs.

Figure 3 shows bidirectional CNNs consisting of two primitive CNNs, which can respond to two directions (from SR_{i-1} to SR_{i+1} and from SR_{i+1} to SR_{i-1}). In the figure, correlation integrators (CIs) that integrate outputs of correlators (C_{x+} and C_{x-}) are employed for obtaining mean local-velocity values. Integrator (CI_i) receives the outputs of the correlators ($C_{x+,i}$ and $C_{x-,i}$) with excitatory and inhibitory weights, and the output of the integrator is given by

$$V_{\mathrm{out},i} = \int_{t_0}^{t_0+\Delta t} C_{x+,i}(t) - C_{x-,i}(t)\, dt, \qquad (1)$$

where t_0 represents the start time of the integration, and Δt the duration of the integration. The output of the integrator is proportional to the mean velocity between time t_0 and $t_0 + \Delta t$.

By arranging bidirectional CNNs along the x- and y-axes, as shown in Fig. 4, we can obtain local velocities by integrating outputs of correlators (C_x, C_y) at each intersection of the CNNs. In the figure, each solid line and allow represent an array of primitive CNNs and preferred direction of the primitive CNN, respectively.

3 A model of direction-selective neural networks

This model is based on scalar-summation of two-dimensional local velocities. We employ the two-dimensional CNNs shown in Fig. 4 for obtaining the

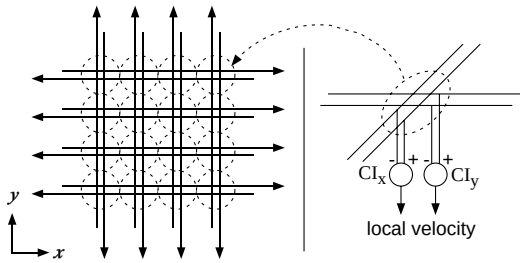

Figure 4: Arrangement of the bidirectional CNNs for obtaining two-dimensional local velocities.

local velocities. Suppose that visual targets move in a two-dimensional plane. In the plane, the luminance-value distribution is defined by $f(x, y, t)$ as a function of spatial position (x, y) and time t. Local velocities of an arbitrary point (x, y) are given by $(u, v) \equiv (dx/dt, dy/dt)$. By regularizing maximum values of u and v to ± 1, we obtain $(u, v) = (\cos\theta, \sin\theta)$, where θ represents the motion direction of the target. Then, we define weighted scalar-summation of these velocities as

$$s = \alpha \cos\theta + \beta \sin\theta, \tag{2}$$

where α and β represent weight strength. Motion direction of a target (θ), which gives maximum values of s, is given by

$$\theta = \begin{cases} \arctan(\beta/\alpha), & (\alpha \geq 0) \\ \arctan(\beta/\alpha) + \pi, & (\alpha < 0) \end{cases} \tag{3}$$

which indicates that a neuron computing scalar value (s) responds selectively to a target moving along a preferred direction. The preferred direction is determined by β/α. Thus, a two-dimensional field of the neurons $s(x, y)$ responds selectively to motion direction according to a spatial distribution of $\beta(x, y)/\alpha(x, y)$.

Among the various weight combinations of α and β, we choose a distribution of $(\alpha, \beta) = (\cos\phi, \sin\phi)$, where ϕ represents the preferred direction of neurons (explained above). Under the given distribution, a neuron outputs

$$s = \cos\phi \cos\theta + \sin\phi \sin\theta, \tag{4}$$

which represents a scalar product of vectors $(\cos\phi, \sin\phi)$ and $(\cos\theta, \sin\theta)$. The scalar product becomes maximum when the direction of the moving target (θ) agrees with that of the preferred direction of the neuron (ϕ). By remapping a distribution of the preferred direction (ϕ) to space as

$$\phi(x, y) = \begin{cases} \arctan(y/x), & (x \geq 0) \\ \arctan(y/x) + \pi, & (x < 0) \end{cases} \tag{5}$$

the preferred direction changes continuously according to the spatial position (x, y). Namely, radial vectors from the origin in the neuron field are equivalent to the preferred direction of the neuron field. In consequence,

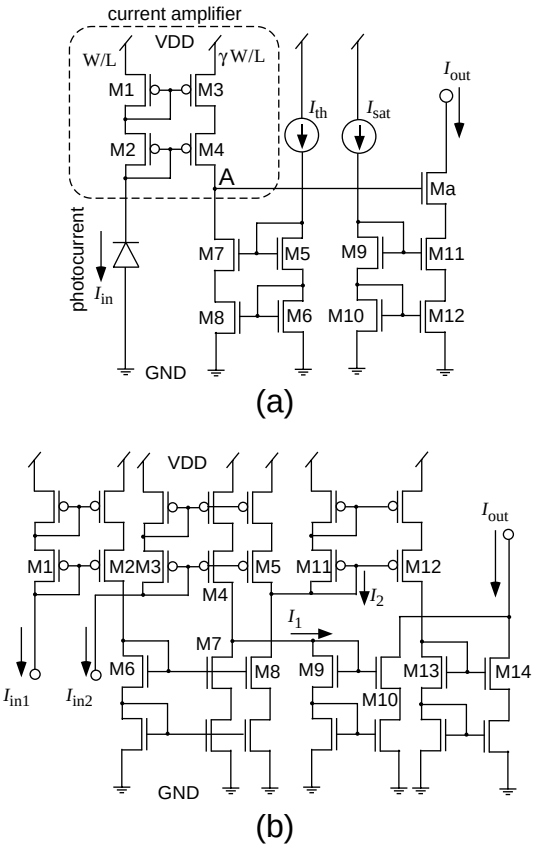

Figure 5: An edge-detection circuit composed of (a) a current amplifier, a current quantizing circuit, and (b) an XOR circuit.

the neuron outputs maximum values when the motion direction of the target (θ) agrees with that of the preferred direction (ϕ).

Here we consider an egomotion of the neuron field instead of moving targets. With the weight strength given in Eqs. (4) and (5), a translation movement can be detected by choosing maximum values of neurons by using winner-take-all networks. Furthermore, the network can detect forward-backward egomotion. In the case of forward motion, all the radial motion vectors start from the origin of the field. These vectors represent the same direction as the preferred direction of the field. Thus, nonzero outputs can be obtained. In the case of backward motion, all vectors head toward the origin. Since the backward direction is opposite to the preferred direction of the field, no output will be obtained.

4 Analog-digital CMOS circuits for motion detection

The analog CMOS motion-detection circuit consists of (i) current amplifiers that amplify incident photocurrents, (ii) current quantizing circuits for image smoothing and quantization of input images, (iii) XOR circuits for detecting edges in the quantized images, and (iv) correlation circuits for detecting local motion.

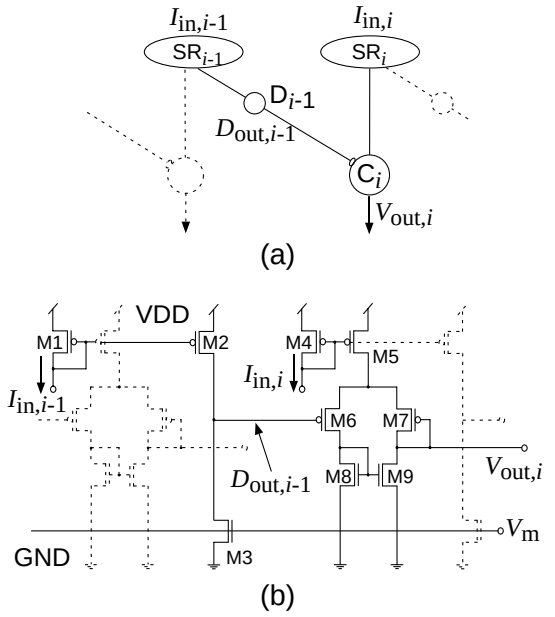

Figure 6: Analog CMOS circuits implementing the primitive CNN: (a) unit cell of the CNN (solid lines); (b) an analog circuit for the unit cell (solid lines).

Figure 5 shows the edge-detection circuit consisting of the current amplifier, the current quantizing circuit, and the XOR circuit. The current amplifier and quantizing circuit are shown in Fig. 5(a). The photocurrent is amplified by a current mirror (M1 through M4) with mirror rate γ. The voltage on node A is nearly equal to zero (or VDD) when the photocurrent is smaller (or larger) than threshold current I_{th}. The voltage is then amplified by transistors M3, M4, M7, and M8 that form a pMOS common-source amplifier. The output current (I_{out}) is limited to I_{sat} by transistors M9 through M12 and Ma. Thus, the circuit outputs zero current (or I_{sat}) when the input photocurrent is smaller (or larger) than I_{th}.

A current-mode digital logic circuit is developed for the XOR operation [Fig. 5(b)]. The circuit receives binary input currents I_{in1} and I_{in2} from the current quantizing circuit (each current is zero or I_{sat}). If $I_{\mathrm{in1}} = I_{\mathrm{in2}} = 0$, the output current of the circuit (I_{out}) is zero because no input currents are given to current mirrors in the circuit. If $I_{\mathrm{in1}} = 0$ and $I_{\mathrm{in2}} = I_{\mathrm{sat}}$, current I_{in2} is copied into M4. The current of M4 is then copied into M9 ($I_1 = I_{\mathrm{in2}}$) and M10, so output current (I_{out}) is equal to I_{in2} ($= I_{\mathrm{sat}}$). If $I_{\mathrm{in1}} = I_{\mathrm{sat}}$ and $I_{\mathrm{in2}} = 0$, current I_{in1} is copied into M11 ($I_2 = I_{\mathrm{in1}} = I_{\mathrm{sat}}$) through M2, M6, and M8. The current of M11 is copied into M14 through M12 and M13, so output I_{out} is equal to I_{in1} ($= I_{\mathrm{sat}}$). If $I_{\mathrm{in1}} = I_{\mathrm{in2}} = I_{\mathrm{sat}}$, output current ($I_{\mathrm{out}}$) is zero because the current of M4 is equal to the current of M7 (therefore $I_1 = 0$) and the current of M5 is equal to the current of M8 (therefore $I_2 = 0$). In consequence, the circuit produces an XOR output from binary input currents I_{in1} and I_{in2} (each is 0 or I_{sat}).

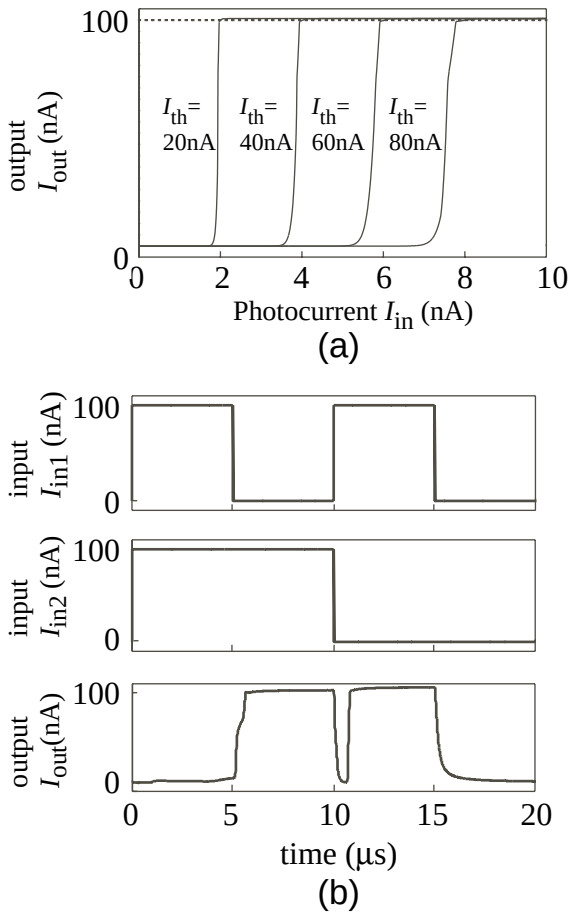

Figure 7: SPICE simulation of (a) a current quantizing circuit and (b) an XOR circuit.

The correlation circuit (CC) corresponding to the primitive CNN is shown in Fig. 6. The unit circuit, which is represented by solid lines in Fig. 6(a), consists of a unity-gain amplifier (M6 through M9) and a pMOS common-source amplifier (M2 and M3). The unity-gain and common-source amplifiers act as the correlator and the delay neuron, respectively, in the CNN [Fig. 6(b)]. When an input current $I_{\mathrm{in},i-1}$, which is larger than the current of M3, is applied to M1, a voltage output appears on node $D_{\mathrm{out},i-1}$ with a time delay resulting from the Miller effect in the amplifier. The delay time can be externally controlled by adjusting common gate-voltage V_{m} of M3. A long (or short) delay is obtained for small (or large) values of V_{m}. The source current of differential pair M6 and M7 is determined by input current $I_{\mathrm{in},i}$ through current mirrors M4 and M5. When the input current ($I_{\mathrm{in},i}$) is applied, the output voltage of the unity-gain amplifier ($V_{\mathrm{out},i}$) is equal to the input voltage ($D_{\mathrm{out},i-1}$). When the input current approaches zero, $V_{\mathrm{out},i}$ also approaches zero, Therefore, the output voltage represents a product-like value of those two inputs; in consequence, the unity-gain amplifier computes a correlation-like value between the values of $I_{\mathrm{in},i}$ and $D_{\mathrm{out},i-1}$.

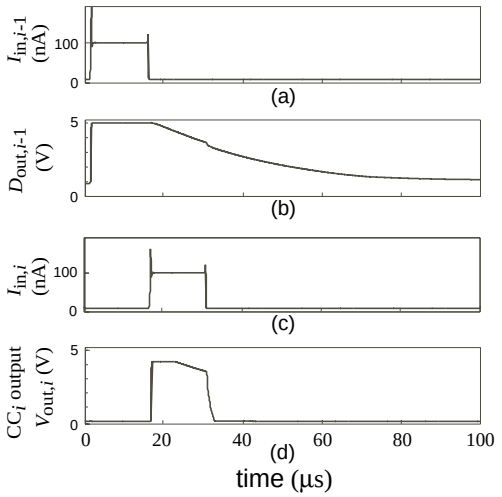

Figure 8: Transient responses of the correlation circuit: (a) input current; (b) delayed voltage produced by the input current; (c) subsequent input current; (d) output of the correlation circuit representing the correlation value between (b) and (c).

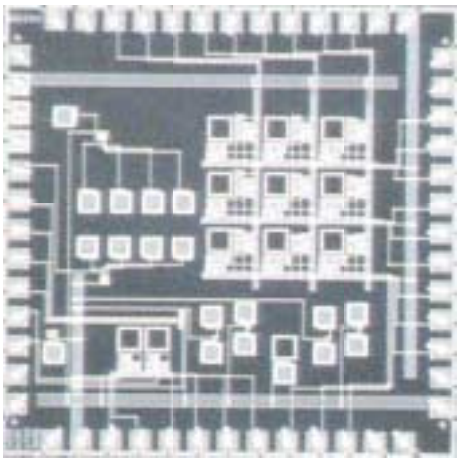

Figure 9: A chip micrograph of a 3×3 matrix of primitive motion-detection circuits.

5 Simulation results

Firstly, we show SPICE simulation results for the motion detection systems introduced in Sect. 2. In the following simulations, we used a typical parameter set for all transistors assuming a 1.2-μm CMOS process.

Figure 7(a) shows static responses of the current quantizing circuit. Supply voltage (VDD), saturation current ($I_{\rm sat}$), and mirror rate (γ) were set to 100 nA, 5 V, and 10, respectively. Threshold current $I_{\rm th}$ was set at 20 nA, 40 nA, 60 nA, or 80 nA. The output of the circuit $I_{\rm out}$ was successfully quantized (0 A to $I_{\rm sat}$) around $\gamma I_{\rm in} = I_{\rm th}$.

Figure 7(b) shows the transient response of the XOR circuit. Square current pulses ($I_{\rm in1}$ and $I_{\rm in2}$) were given to the circuit as shown in the figure (top and middle). The resultant output current of the circuit is shown in the same figure (bottom). The output was logical "0" when $I_{\rm in1} = I_{\rm in2}$ and logical "1" when $I_{\rm in1} \neq I_{\rm in2}$, so the expected XOR operation was obtained. A slight delay of a few microseconds was observed in the response, but this is not a problem in the circuit operation.

Figure 8 shows transient responses of the CC in Fig. 6(b). Supply voltage (VDD) and $V_{\rm m}$ were set at 5 V and 0.45 V, respectively. In the simulations, input currents of CCs were given by XOR circuits. First, the input current was applied to CC_i [$I_{{\rm in},i-1}$ in Fig. 8(a)], and the corresponding delayed voltage ($D_{{\rm out},i-1}$) was produced [Fig. 8(b)]. Then, a subsequent current ($I_{{\rm in},i}$) was applied to CC_i, as shown in Fig. 8(c). From delayed voltage $D_{{\rm out},i-1}$ and applied input $I_{{\rm in},i}$, the CC_i calculated correlation voltage $V_{{\rm out},i}$, which was approximately proportional to $I_{{\rm in},i} \times D_{{\rm out},i-1}$ as shown in the figure. When the light spot (edge) moves at a constant velocity, the local velocity is represented by an inverse of the width of the output pulses. Therefore, the local velocity can be approximately obtained as an inverse value of the temporal integration of the correlation voltage as given in Eq. (1). In the simulaiton, the calculated total-power dissipation was 3 μW.

We fabricated a prototype LSI by using a 1.2-μm double-poly double-metal CMOS process. Figure 9 shows a chip micrograph of the motion-detection circuits. The chip contains 3×3 matrix of primitive motion-detection circuits. The current amplifiers, the quantizing circuits, and the XOR circuits were fabricated in another chip.

Figures 10 and 11 show numerical simulations of the direction-selective neural networks described in Sect. 3. In the simulation, the weight strength of the network was configured according to Eqs. (4) and (5). Firstly, two-dimensional local velocities (u, v) were obtained from bidirectional CNNs with moving light bars [Figs. 10(a) and 11(a)]. Then, distributions of maximum outputs of the neurons $Max_t[s(x, y)]$ were calculated [Figs. 10(b) and 11(b)]. When the bar moved rightward along a line $y = 0$ ($\theta = 0$) [Fig. 10(a)], neurons on a line $y = 0$ $(x > 0)$ outputted maximum values among the neuron field ($\phi = 0$). On the other hand, when the bar moved along a line $y = x$ ($\theta = \pi/4$) [Fig. 11(a)], neurons on a line $y = x$ $(x > 0)$ outputted maximum values ($\phi = \pi/4$) as expected.

6 Summary

We have developed compact CMOS circuits for practical motion-detection systems with direction-selective neural networks. Basic operations of edge-detection circuits and motion-detection circuits were confirmed by SPICE.

The developed direction-selective neural network model has the following advantages: first, the correlation neural networks employed in the model are suitable for hardware implementation because of the compact circuit structure and low-power dissipation; sec-

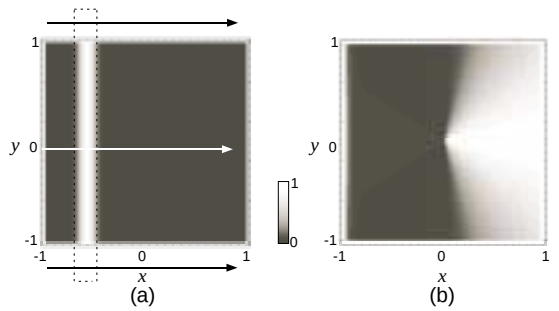

Figure 10: Numerical simulation of proposed direction-selective neural networks with a moving light bar along a line $y = 0$. (a) Input field and target; (b) resultant maximum-response distribution of the neuron field.

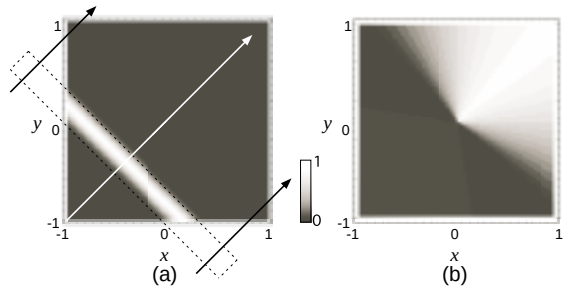

Figure 11: Simulation results for the direction-selective neural networks with a moving light bar along a line $y = x$. (a) Input field and target; (b) resultant maximum-response distribution of the neuron field.

ond, a simple scalar summation operation can perform the direction-selective neural field; third, the model can detect egomotions by means of additional winner-take-all neural networks.

References

[1] D. H. Ballard and C. M. Brown, *Computer vision*. Prentice-Hall, Inc., New Jersey, 1982.

[2] P. K. B. Horn and G. B. Schunck, "Determining optical flow," *Artif. Intelli.*, vol. 17, pp. 185-203, 1981.

[3] T. Poggio, W. Yang, and V. Torre, *The computing neuron*. Addison Wesley, New York, 1989.

[4] J. Hutchinson, C. Koch, J. Luo, and C. Mead, "Computing motion using analog and binary resistive networks," *Computer*, vol. 21, pp. 52-63, 1988.

[5] J. Tanner and C. Mead, "An integrated analog optical motion sensor," *VLSI signal processing II*, vol. 21, pp. 59-76, 1987.

[6] R. Douglas, M. Mahowald, and C. Mead, "Neuromorphic analogue VLSI," *Annu. Rev. Neurosci.*, vol. 18, pp. 255-281, 1995.

[7] C. Mead, *Analog VLSI and neural systems*. Addison Wesley, New York, 1989.

[8] T. S. Lande, *Neuromorphic systems engineering: neural networks in silicon*. Kluwer Academin Publishers, 1998.

[9] R. Dudley, *The biomechanics of insect flight. form, function, evolution*. Princeton, New Jersey, 2000.

[10] B. J. Sheu and J. Choi, *Neural information processing and VLSI*. Kluwer Academic Publishers, Boston, 1995.

[11] D. C. Carroll, N. J. Bidwell, S. B. Laughlin, and E. J. Warrant, "Insect motion detectors matched to visual ecology," *Nature*, vol. 382, pp. 63-66, 1996.

[12] W. Reichardt, *Principles of Sensory Communication*. Wiley, New York, 1961.

[13] R. Kern, M. Egelhaaf, and M. V. Srinivasan, "Edge detection by landing honeybees: behavioural analysis and model simulations of the underlying mechanism," *Vision Res.*, vol. 37, pp. 2103-2117, 1997.

[14] J. Kramer, R. Sarpeshkar, and C. Koch, "Pulse-based analog VLSI velocity sensors," *IEEE Trans. Circuits and Systems II*, vol. 44, pp. 86-101, 1997.

[15] T. Delbr̈uck, "Silicon retina with correlation-based, velocity-tuned pixels," *IEEE Trans. Neural Networks*, vol. 4, pp. 529-541, 1993.

[16] T. Asai, M. Ohtani, and H. Yonezu, "Analog MOS circuits for motion detection based on correlation neural networks," *Jpn. J. Appl. Phys.*, vol. 38, pp. 2256-2261, 1999.

[17] M. Ohtani M, H. Yonezu, and T. Asai, "Analog MOS IC implementation of motion-detection network based on a biological correlation model," *Jpn. J. Appl. Phys.*, vol. 39, pp. 1160-1164, 2000.

[18] T. Asai, M. Koutani, and Y. Amemiya, "An analog-digital hybrid CMOS circuit for two-dimensional motion detection with correlation neural networks," in *International joint conference on neural networks*, 2000, WC7-NN0353.